J Mater Sci (2012) 47:949–959
DOI 10.1007/s10853-011-5874-0

Tensile strength of windmill palm (*Trachycarpus fortunei*) fiber bundles and its structural implications

Shengcheng Zhai · Dagang Li · Biao Pan · Junji Sugiyama · Takao Itoh

Received: 8 June 2011 / Accepted: 11 August 2011 / Published online: 24 August 2011

Abstracts *Trachycarpus fortunei* (windmill palm) is one of the most widely distributed and widely used palms in East Asia. In order to find further uses for the palm's fibers, however, more information on their mechanical and anatomical properties is needed. With this in mind, tensile strength and Young's modulus of windmill palm fiber bundles were investigated and the structural implications considered. The anatomical features in cross-section, the fracture mode, and the microfibril angle (MFA) of natural fiber bundles were determined. The transverse sectional area occupied by fibers in a fiber bundles (S_F) contributes to mechanical strength in practice. It was found that the ratio of S_F to the transverse sectional area of a fiber bundle dramatically increases with a decrease in bundle diameter. Therefore, tensile strength and Young's modulus of an individual fiber bundle in this species increase in parallel with a decrease in fiber bundle diameter. The observed MFA features might have a relationship with the biomechanical movements of fiber bundles in the windmill palm. The potential uses of windmill palm fibers have been discussed.

S. Zhai · D. Li · B. Pan · T. Itoh
College of Wood Science & Technology, Nanjing Forestry University, Nanjing, China

S. Zhai (✉) · J. Sugiyama
Laboratory of Biomass Morphogenesis and Information, Research Institute for Sustainable Humanosphere, Kyoto University, Gokasho, Uji, Kyoto 611-0011, Japan
e-mail: zhai_sc@rish.kyoto-u.ac.jp

T. Itoh
Nara National Research Institute for Cultural Properties, Nara, Japan

Abbreviations

S_F Transverse sectional area occupied by fibers
S_V Transverse sectional area occupied by vessels and phloem tissue

Introduction

Palmae (Arecaceae) is an important taxon of the monocotyledon and plays an essential role in the daily lives of millions of people in tropical and subtropical regions [1–5]. The properties and commercial utilization of palms are dependent on their structural and mechanical characteristics. There are many publications on the oil palm (*Elaeis guineensis*), the wine palm (*Caryota urens*), and the coconut palm (*Cocos nucifera*), etc. [6–17]. However, the windmill palm (*Trachycarpus fortunei*), which is the most common species in East Asia and is distributed throughout temperate and tropical zones, has yet to be thoroughly investigated. The recent work of Windsor-Collins et al. [18] obtained data on the resistance to torsion versus the shape factor of petioles taken from *T. fortunei*. Insight has thus been gained into the mechanical behavior of the *T. fortunei* palm petioles. Windmill palm fibers have mainly been used for making thatch, marine rope, and traditional raincoats. According to the *Bencao gangmu*, a Ming Dynasty (1368–1644) meteria medica [19], people living long ago already knew that windmill palm fibers were well-suited for making rope that could be used in wet conditions for hundreds of years without showing signs of

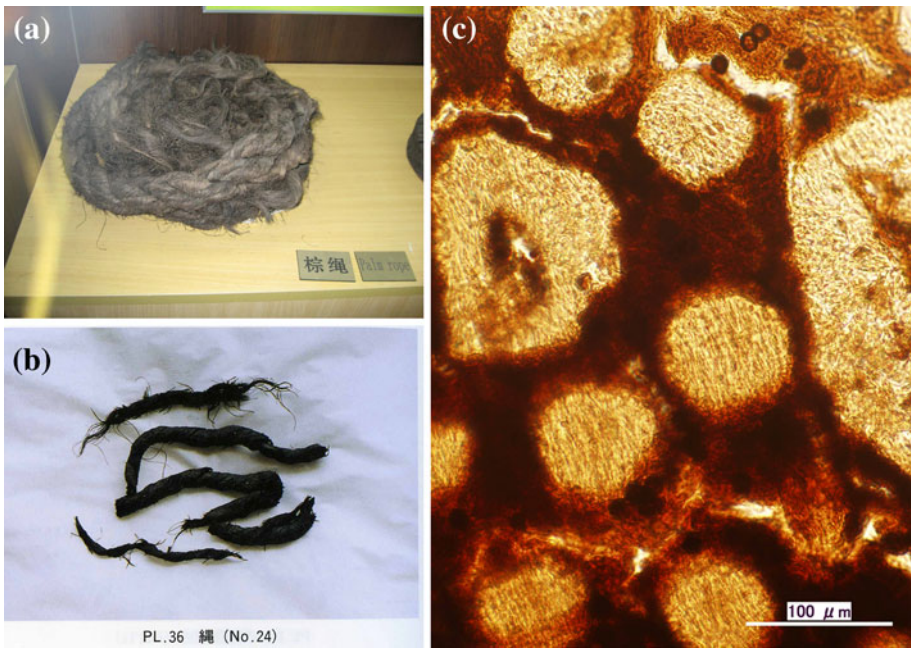

Fig. 1 Objects excavated from archeological sites testifying to utilization of windmill palm fibers in ancient times: **a** windmill palm fiber rope more than 8 cm in diameter from a Ming Dynasty (1368–1644) shipyard site, **b** rope recovered from the seabed off Takashima Island, where the Yuan Dynasty (1279–1368) fleets of Kublai Khan sank, **c** cross-section of Takashima Island rope fibers, identified as being windmill palm fibers

decay. Archeological excavations [20, 21] (Fig. 1) have indeed validated such claims.

Although leaves originate from the stem, fibers for utilization are usually collected from the well-lignified leaves surrounding the windmill palm stem, rather than from the stem. The windmill palm stem is surrounded by many layers of leaves and the fiber bundles in a leaf sheath are separated from each other when the parenchyma tissue disintegrates as the fiber bundles mature and lignify (Fig. 2). The fiber bundles in a leaf provide a good model for understanding the physical properties (or strength) of the windmill palm. On the contrary, it is absolutely impossible to measure the physical strength of intact fiber bundles distributed in the palm stem. However, it can be estimated fairly precisely by measuring the physical properties (or strength) of fiber bundles in the leaf sheath. Therefore, these estimations not only contribute to the utilization of the palm stem but also may lead to an understanding of the physical properties of the whole stem.

In general, the mechanical properties of plant fibers derive from such physical, chemical, and morphological characteristics as crystalline structure, density, cellulose content, microfibril orientation, and fiber bundle diameter. Satyanarayana et al. [13] tested fibers from various parts of the coconut tree. Zhang et al. [22] measured the tensile strength of some natural fibers such as jute and wood. Subsequently, Munawar et al. [23] investigated physical and mechanical properties of fibers from several non-woody plants. They compared tensile strength to fiber bundle diameter. According to these papers, the tensile strength of fiber bundles with a small diameter was larger than that of fiber bundles with a larger diameter. Why do natural fibers show such a characteristic? If the characteristics of fiber bundles are the same, the tensile strength of

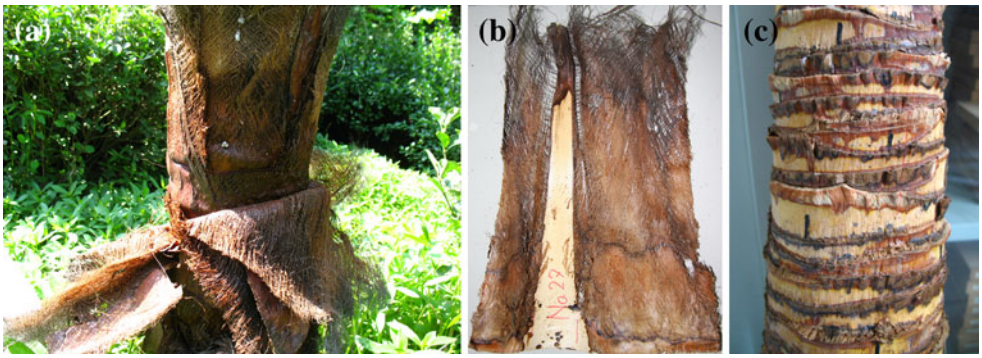

Fig. 2 Photographs of windmill palm showing lignified fiber bundles in leaf and stem: **a** windmill palm stem surrounded by many layers of leaf sheaths (at a height of 1.5 m), **b** one leaf sheath taken from a windmill palm, **c** windmill palm stem after all leaves have been pilled

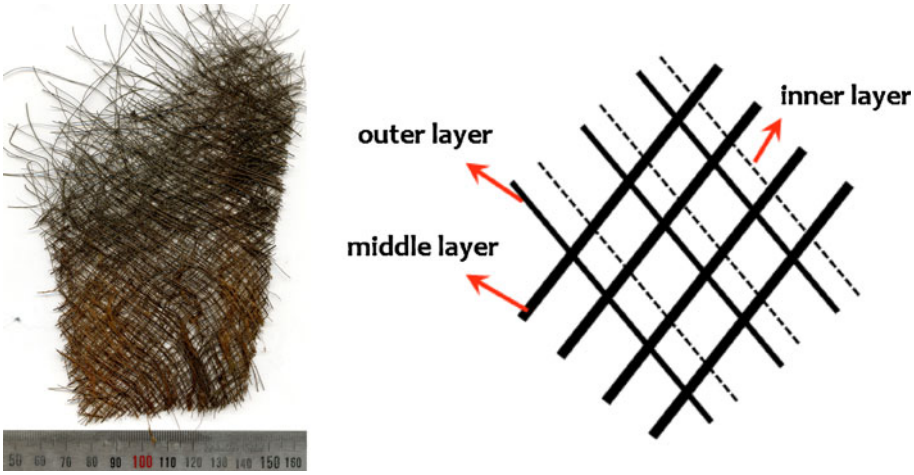

Fig. 3 Graphs of leaf sheath taken from windmill palm. *Left* a small piece of one sheet of leaf sheath with scale (cm). *Right* a model of fiber bundles' variance in one sheet of leaf sheath. The different layers of fiber bundles are characterized by differences in diameter, orientation, and location

bundles of different diameters should be the same. Until now no clear answer to this question has been given. Meanwhile, the structure and mechanics of the fiber caps of different types of vascular bundles from the Mexican fan-palm (*Washingtonia robusta*) were studied [24, 25]. It was found that gradients in stiffness appeared across the fiber caps in the center of the trunk, whereas stiffness remained high across the caps in the periphery of the trunk. This was attributed to the anatomy of the fiber caps of three different types of vascular bundles.

This article focuses on mechanical properties resulting from the internal structure of windmill palm fibers. The influence of anatomical structure variations and ultra-structure differences in windmill palm fibers are discussed. New evidence was obtained demonstrating why small fiber bundles, as compared to large ones, show high tensile strength and high Young's modulus.

Materials and methods

Sample preparation

Fiber bundles were obtained from the leaf sheaths of a windmill palm of approximately 10 m in height. Leaf sheaths were hand-picked from the windmill palm at a height of 1.5 m from the ground (Fig. 2a). Each sheath is composed of an outer, middle, and inner layer, and, each layer contains fiber bundles of different diameters, orientations, and locations. The fiber bundles with the largest diameter are found in the middle layer, those with a middle-sized diameter are found in the outer layer, and those with the smallest diameter are found in the inner layer (Fig. 3). Before being collected, fiber bundles were rinsed many times in rain water and then dried. A side from this and gently removing the dust from the surface of the fiber bundles, no other treatment was done to the hand-picked fiber bundles.

Microscopic observation and imaging quantification

After collecting many sheets of leaf sheaths composed of mature vascular bundles (or fiber bundles), the diameters of the individual fiber bundles in the three layers were measured by means of a digital optical microscope (Micro Square, DS-3USV, RAS Machine Tool Technologies, Inc., USA). In order to confirm the presence of three layers in each sheet of leaf sheath, a part of a leaf sheath taken from an unlignified area (Fig. 4a) was embedded in celloidine. Transverse and longitudinal sections with a thickness of 20–30 μm (Fig. 4b, c) were made by means of a sliding microtome (Yamato Kohki Industrial Co. Ltd., Japan, TU-213).

In each layer of one sheet of leaf sheath, five to ten fiber bundles were bound tightly together by cotton threads, cut into a 5 mm length, and embedded in epoxy resin. From these resin-embedded specimens, semi-thin sections were cut using a semi-thin microtome (Leica, RM2145, Germany). Some of the transverse sections were stained with safranin in order to observe the lignified tissue more clearly. The sections were observed under transmitted- and polarized-light microscopes (Ortoplan, Leitz Wetzlar, Germany).

Microscopes equipped with a LCD OLYMPUS video camera (model DP70) were used to resolve images. These images were used for quantitative analysis in order to obtain such basic data on palm fiber bundles as the amount of transverse sectional area occupied by fiber in a fiber bundle (S_F), the amount of transverse sectional area occupied by vessels and phloem tissue in a fiber bundle (S_V) (Fig. 5), the amount of single fiber in a fiber bundle, and the thickness and diameter of a single fiber wall. Measurements were carried out using the Motic Images image analysis software. Quantitative characteristics were determined by means of photographs that have been previously obtained using an image analysis system. Only those with fully visible fiber bundle cross-sections were used [26].

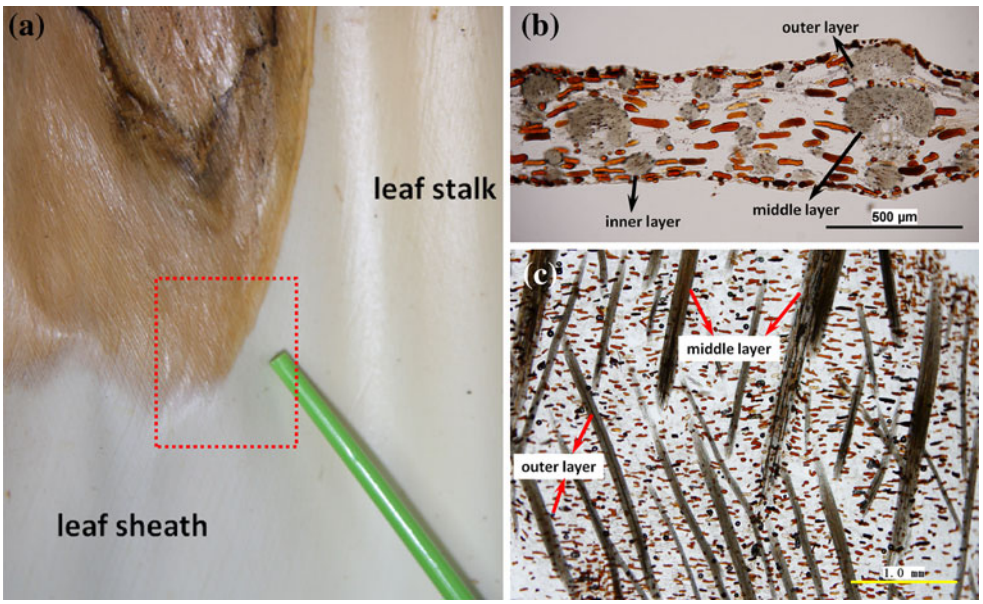

Fig. 4 Layered arrangement of fiber bundles in one sheet of leaf sheath: **a** sample of unlignified leaf sheath for celloidine embedding, **b** transverse section of leaf sheath, **c** longitudinal section of leaf sheath

Tensile strength test

In order to test tensile strength, the fiber bundles in a leaf sheath were air-dried until their moisture content ranged from 8 to 10% by weight (wt%). After cutting the fiber bundles into 20–25 mm lengths (Fig. 6a), the fibers were fixed to 10 mm gauge length paper frames using two-part epoxy adhesives (Rapid Araldite AR-R30, Nichiban Co. Ltd., Japan) as shown in Fig. 6b, in accordance with the preparation procedure mentioned in the ASTM D 3379-75 standard [23, 27, 28]. Then, at ten randomly selected points, the diameter of each fiber bundle was measured using a digital optical microscope with either 150 or 300 times of magnification, depending on the diameter of the fiber bundles. Following the calculation method of Munawar et al. [23], the transverse sectional area of the fiber bundles was determined by using the circle equation based on an average value of diameter measurements taken at ten locations. A mean diameter was used to calculate a fiber's transverse sectional area, which is an important parameter for determining fiber tensile strength.

Following to the standard ASTM D-882-75b, a universal testing machine (Instron, 4411, Instron Corporation, Canton, MA, USA) was used to test the tensile strength of fiber bundles. The crosshead speed was kept at 1 mm/min in all tests. Before testing tensile strength, the middle part

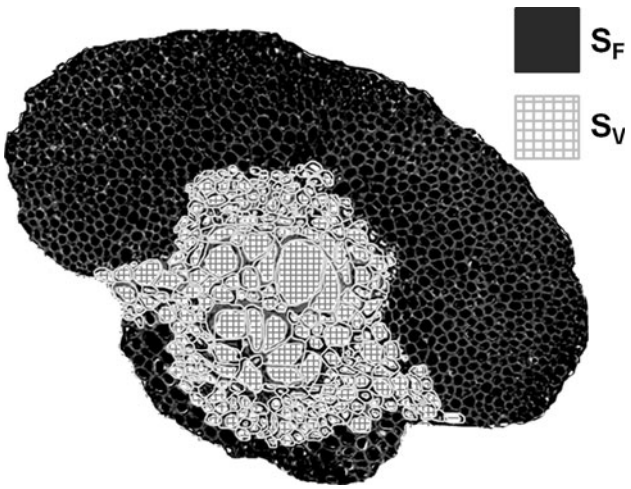

Fig. 5 Illustration showing areas of S_F and S_V in a fiber bundle of the windmill palm. S_F transverse sectional area occupied by fibers in a fiber bundle, S_V transverse sectional area occupied by vessels and phloem tissue in a fiber bundle

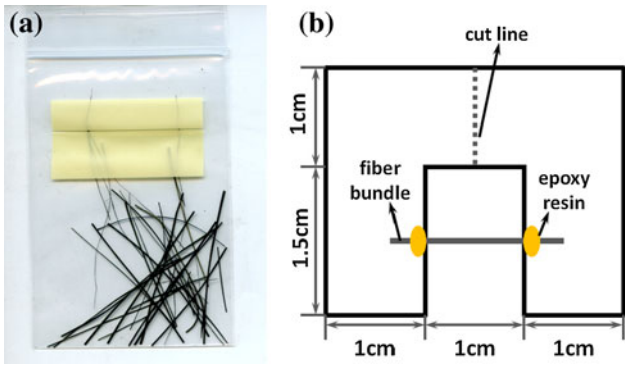

Fig. 6 Illustration of fiber bundles (**a**) and paper frame support used for tensile strength test (**b**). A fiber bundle is fixed on the paper frame by means of epoxy adhesive. The paper is then cut in two along the dotted line, and the paper supports are pulled apart

of the supporting paper frames was cut as shown in Fig. 6b. Palm fiber bundles for the tensile strength test were also separated into three groups based on what layer they occupied in the leaf sheath. In order to obtain effective statistical data, 70 fibers from each group were tested. The fiber bundles that were fractured at the end of the paper frame next to the glue clamp were excluded from the test results. Measurements were made at 70% relative humidity (r.h.) and 25 °C.

A preliminary test using a universal testing machine was done with a load (max. load 5 N). Because the maximum load carrying capacity of fibers in the middle layers was over 5 N, the load was changed to 50 N throughout the present experiments. After the tensile strength test was carried out, the fractured surfaces of some palm fiber bundles were observed under scanning electron microscope (Hitachi Co. Ltd., TM1000, Japan).

X-ray diffraction measurement

X-ray diffraction profiles of windmill palm fibers were collected. Typical fiber bundles were taken from the three different layers in a leaf sheath for testing. X-ray diffraction diagrams were obtained using a vacuum camera mounted on a Rigaku RU-200BH rotating anode X-ray generator. The main experimental conditions were Cu Kα radiation ($\lambda = 1.54$ Å), tube voltage 50 kV, tube current 100 mA. X-ray diffraction patterns were recorded on Fuji Imaging Plates (BAS-IP SR 127) [29–32]. From the X-ray diffraction pattern obtained, using Image J image analysis software, the mean MFA of palm fibers was determined based on azimuthal intensity distribution of cellulose 200 reflections. Secondary, equatorial profiles were obtained by radial integration of the diagram, where the Gaussian functions were fitted to crystalline peaks. The relative crystallinity index (CrI) was determined from the ratio of the separated peak area to the total area [33, 34].

Results and discussion

Structure of fiber bundles

The difference in the diameters of the fiber bundles from both transverse and longitudinal sections of the celloidine embedded samples was observed. The fiber bundles in the middle layer were larger than those in the outer and inner layers (Fig. 4b, c). A series of statistical data obtained using a digital optical microscope showed that the fiber bundles in the middle layer had a mean diameter of 418.0 μm, while those of the bundles in the inner and outer layers were 202.1 and 342.5 μm, respectively. The divergence of diameter in fiber bundles taken from different layers is shown in Fig. 7.

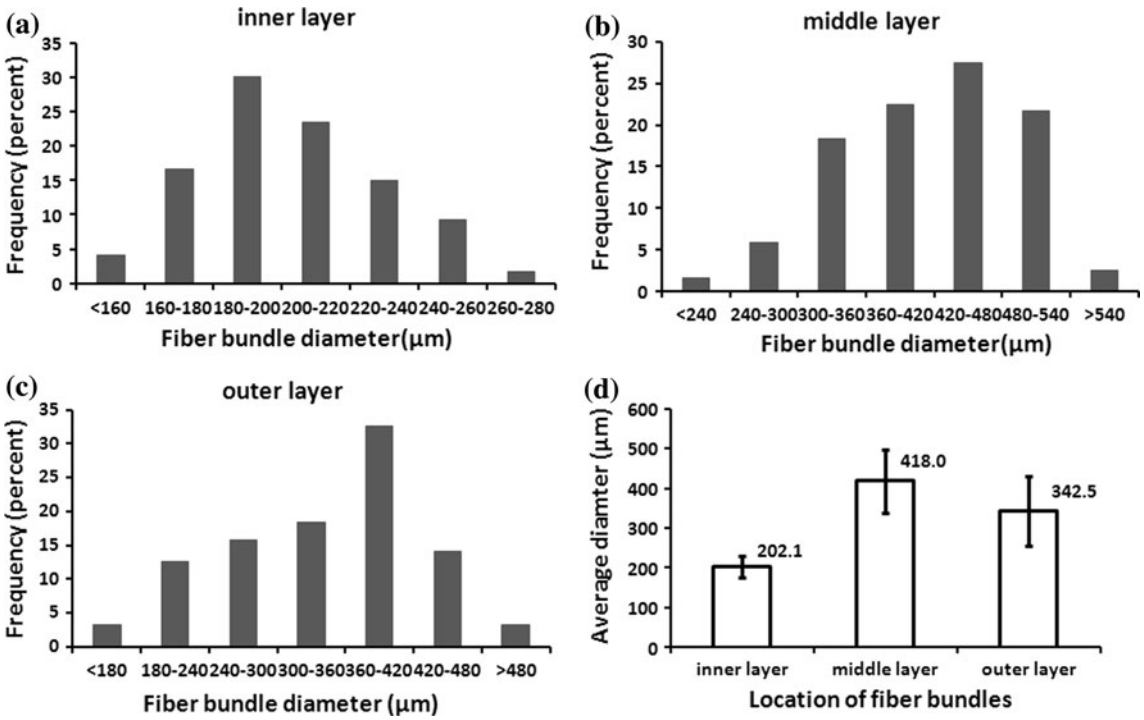

Fig. 7 Diameter distributions of fiber bundles among three layers in one sheet of leaf sheath. Fiber bundles from inner layer (**a**), middle layer (**b**), and outer layer (**c**) with remarkable difference in average diameter (**d**)

Literature showed that Sisal aggregates (*Agava sisalana*) was 100–400 μm in diameter [35]; the typical diameter of coir fiber bundles from the coconut palm (*Cocos nucifera*) was about 200 μm [36]. Satyanarayana et al. [13] measured the diameters of the coconut palm tree's fiber bundles, and they also separated the fiber bundles into three groups a *thick group*, a *thin group* and a *middle group*—which were located in one sheet of leaf sheath. According to their paper, the diameter of the thick group's fiber bundles was 1100–1600 μm, while those of the thin and middle groups' fiber bundles were 300–600 and 300–1000 μm. Comparing these data with our results, it can be noticed that fiber bundles in the outer layer of our definition corresponded to the *middle group*, the middle layer to the *thick group*, and the inner layer to the *thin group*.

When focusing on one fiber bundle, the transverse sections of the safranin-stained fiber bundles clearly revealed lignified tissue. The fiber bundles in the inner layer were almost completely composed of fibers (Fig. 8a), while the fiber bundles in the middle and outer layers showed clear vessels and phloem tissue occupying substantial amount of their transverse sectional area (Fig. 8b, c). Figure 8 also shows that S_F was the largest in the middle layer, followed by the outer and inner layers. At the same time, S_V was also the largest in the middle layer followed by the outer and inner layers, although it was not easy to observe S_V in fiber bundles from the inner layer.

Figure 9a shows a transverse sectional image of the fiber bundles in the inner layer as observed by transmitted-light microscope. When the same fiber bundles were observed under polarized-light, the amount of vessels and phloem tissue could be clearly seen as a dark region near the center of each individual fiber bundle (Fig. 9b). It was clear that fiber bundles consisted of a large number of fibers and a negligible amount of vessels and phloem tissue. The evidence indicates that no fiber bundle consists only of fibers. Even fiber bundles with a small diameter also have vessels and phloem tissue.

With this in mind, S_F and S_V in a fiber bundle, the number of fibers in a bundle, fiber diameter, and fiber wall thickness were measured in each of the three layers of one leaf sheath. Table 1 shows that the mean fiber diameter and fiber wall thickness were similar in fiber bundles taken from different layers of one leaf sheath. In this case, the characteristics of a single fiber are almost the same among the different fiber bundles.

Mechanical properties

After tensile strength was tested, typical stress–strain curves for fiber bundles from different layers in one leaf sheath were obtained (Fig. 10). The curves showed a yielding, followed by plastic deformation until breakage from 30 to 60% strain for fiber bundles. The line of

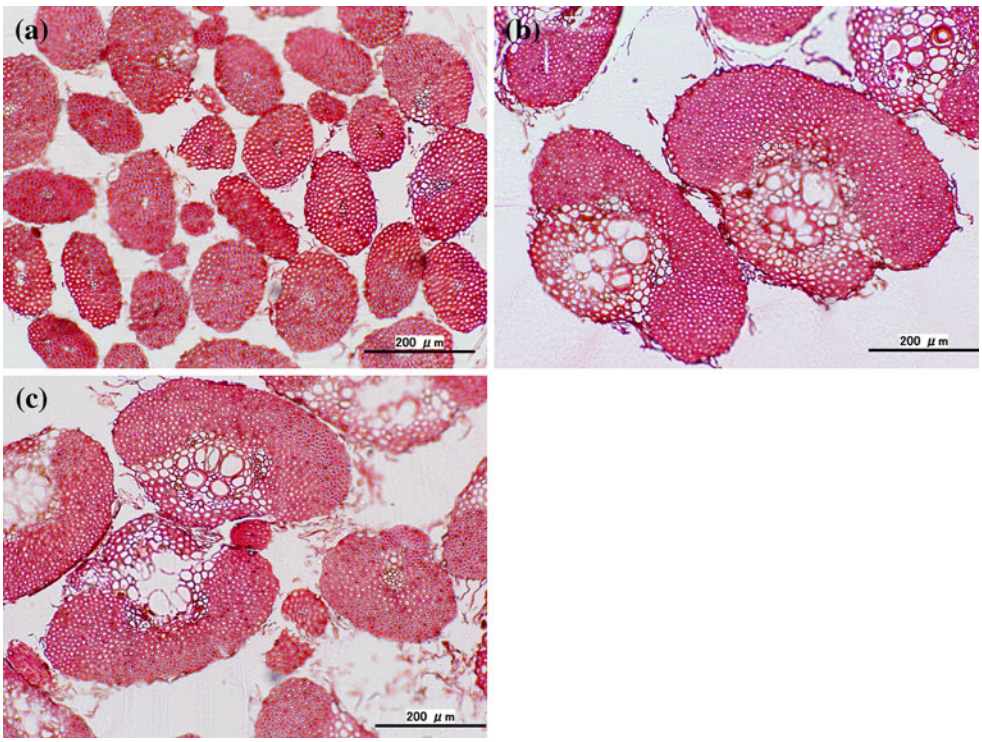

Fig. 8 Transverse sections of fiber bundles taken from inner (**a**), middle (**b**), and outer layers (**c**) of one sheet of leaf sheath, showing vessels and phloem tissue accompanied by fibers in each fiber bundle

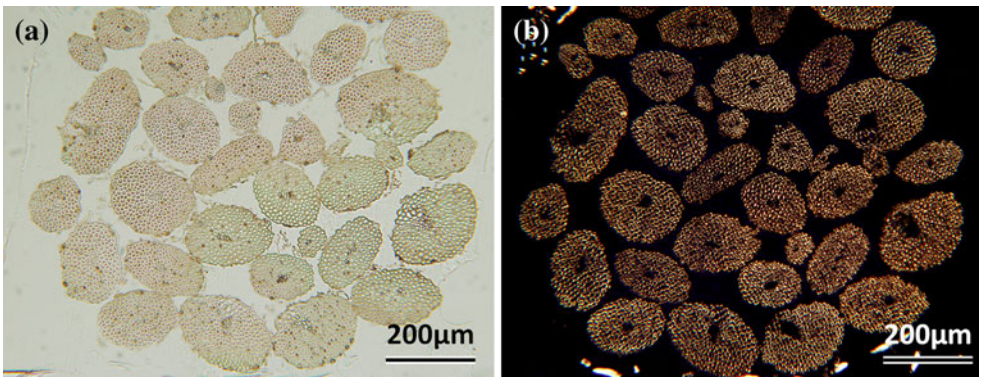

Fig. 9 Transverse sectional image of fiber bundles in the inner layer observed by transmitted- (**a**) and polarized-light (**b**). The noticeable dark region near the center of each fiber bundle in (**b**) is the area occupied by vessels and phloem tissue

Table 1 Fiber characteristics of different layers of one sheet of windmill palm leaf sheath

Leaf sheath layer	Inner	Middle	Outer
Area occupied by fibers (S_F) (100 μm^2)	~193	~715	~589
Area occupied by vessels and phloem (S_V) (100 μm^2)	~13	~358	~279
Number of fibers in one bundle	~160	~840	~590
Fiber diameter (μm)	10.4 (±0.4)	9.5 (±0.5)	10.1 (±0.4)
Fiber wall thickness (μm)	2.2 (±0.16)	2.1 (±0.25)	2.1 (±0.16)

breakage in the fiber bundles mainly ran perpendicular to the direction of the tensile stress. Table 2 presents the mechanical properties of fiber bundles in the three different layers taken from one windmill palm leaf sheath. Although the diameter of the inner layer was the smallest among the three layers, the fiber bundles from the inner layer showed higher tensile strength (113.72 MPa) and Young's modulus (1249.70 MPa) than did the fiber bundles in the other layers. The plots of the mechanical properties of tensile strength and Young's modulus versus diameter of fiber bundle from the windmill palm are shown in Fig. 11. With these plots, the variation in mechanical properties can be

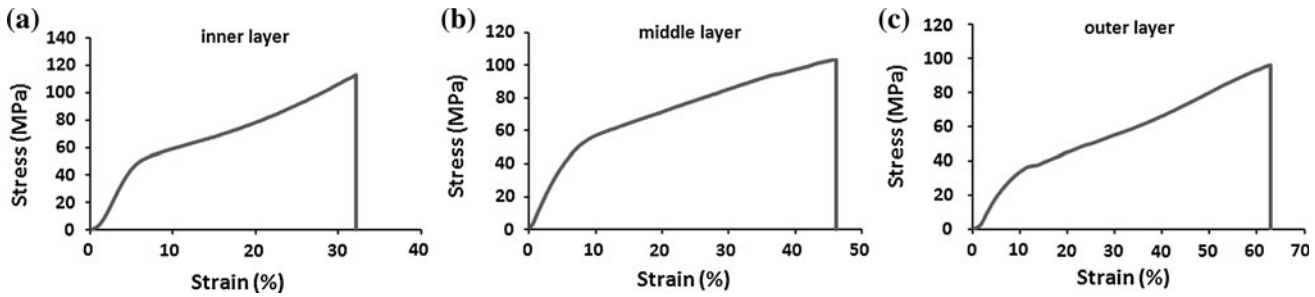

Fig. 10 Typical stress–strain curves of fiber bundles taken from the inner (**a**), middle (**b**), and outer (**c**) layers of one sheet of windmill palm leaf sheath

Table 2 The mechanical properties of fiber bundles from different layers of one sheet of windmill palm leaf sheath ($n = 70$, test speed = 1 mm/min)

Layer	Max. load (kN)			Modulus (MPa)			Max. str (MPa)			BRK.%STN (%)		
	Mean	SD	C.V. (%)	Mean	SD	C.V. (%)	Mean	SD	C.V. (%)	Mean	SD	C.V. (%)
Inner	3.45	0.83	24.18	1249.70	382.58	30.61	113.72	25.11	22.08	39.52	15.69	39.70
Middle	12.25	4.02	32.77	778.93	332.67	42.71	91.93	32.42	35.27	55.20	20.77	37.62
Outer	7.40	2.79	37.62	817.11	388.57	47.55	82.08	30.23	36.83	47.52	22.32	46.98

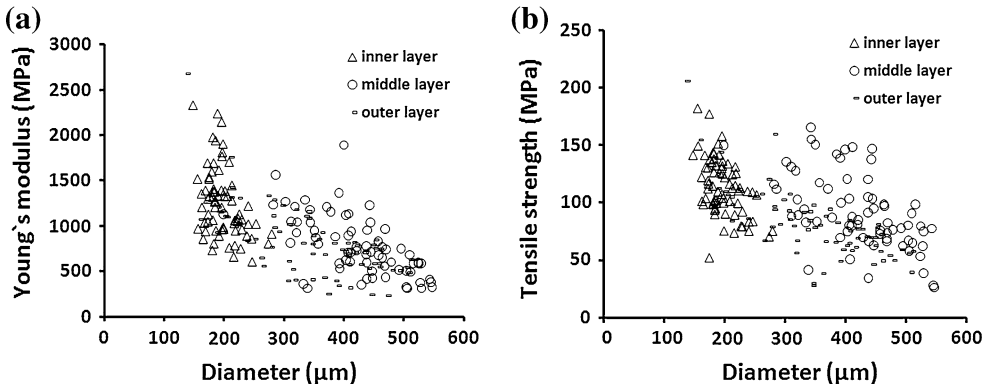

Fig. 11 Relationship between diameter and Young's modulus (*left*), and diameter and tensile strength (*right*) of windmill palm fiber bundles

evaluated. They show a decreasing trend in tensile strength and Young's modulus with an increasing trend in the diameter of the fiber bundles in the three different layers and vice versa.

Munawar et al. [23] investigated the physical and mechanical properties of seven non-woody plant fiber bundles such as abaca leaf fibers, pineapple leaf fibers, sisal leaf fibers, coconut husk fibers, and bast fibers of kenaf and ramie. The authors concluded that the tensile strength and Young's modulus showed a decreasing tendency with an increase in the diameter of the fiber bundles. Some previous papers have also described a similar relationship between diameter and tensile strength as well as Young's modulus in flax fibers [37] and jute fibers [22]. However, no clear reasons were presented in these papers to explain these phenomena. A similar phenomenon in the fiber bundles taken from the windmill palm was confirmed in this study. Especially, the inner-layer fiber bundles, which had the smallest diameters, showed the highest tensile strength among the three layers. If the fiber cell walls were thicker and the fiber diameters smaller in the inner layer than in the other layers, such a phenomenon as mentioned above could occur. However, as the results in Table 1 show, both fiber diameter and fiber cell wall thickness did not show any substantial differences in the three layers of fiber bundles. Therefore, instead of anatomical features, more attention was paid to the different tissue types involved in a vascular bundle: that is, fibers, vessels, and phloem tissue.

The presence of fibers predominantly contributes to the mechanical strength of the fiber bundles (or vascular bundles), while the presence of vessels and phloem tissue tends to reduce mechanical strength. Fiber bundles in one sheet of leaf sheath taken from the windmill palm were divided into three layers according to their size, orientation, and location. As mentioned before, S_V was largest in the *middle layer*. It decreased dramatically in the inner layer of a mature leaf sheath. The vascular bundle in the *inner layer* of a leaf sheath did not show a substantial value of S_V. However, the mean tensile strength and Young's modulus of the vascular bundles in the *inner layer* of a leaf sheath were the largest of the three different layers. Therefore, the only parameter that contributes to the mechanical properties of fiber bundles was the ratio of S_V in one bundle. In the inner layer, S_V was about 1300 μm^2 and just 6–7% of one fiber bundle's transverse sectional area (Table 1). However, S_F in the middle layer was 71500 μm^2, while S_V was 35800 μm^2. S_V increased to 33% of transverse sectional area. These findings strongly suggest that the tensile strength of a fiber bundle increases in accordance with a decrease of S_V, which occurs with an increase in fiber bundle diameter. Considering the structural and mechanical properties of the component cells in a fiber bundle, it was found that S_V in a transverse sectional area of a fiber bundle was an important factor affecting fiber bundle tensile strength.

The tensile properties of various natural fibers, along with the results obtained here on windmill palm fiber bundles, are summarized in Table 3 for better comparison [13, 28, 38]. The tensile strength and modulus of windmill palm fiber bundles are usual for natural fibers. The elongation at break percentage is much higher than that of the other plants referred to in Table 3. Composite materials having a too low elongation to break will be brittle. Therefore, the windmill palm will be a good natural resource for enhancing the strength and stiffness of composite materials.

To make sure there was zero or insignificant, slippage at normal conditions of tension, the fracture surface of broken fiber bundles was observed under SEM. In Fig. 12, representative SEM micrographs of windmill palm fiber bundles' fracture surface are presented. No epoxy resin penetrated the testing length of fiber bundles—a condition that, as other researchers have mentioned [39],—may strengthen the mechanical properties of the fiber bundles tested. The morphology of windmill palm fiber bundles can also be characterized. The tubular cells are oriented parallel with the bundle axes. No specimens were found in which fiber bundles were visibly pulled out in the proximity of the interface of fiber bundles and epoxy resin. In the view of

Table 3 Properties of windmill palm fiber bundles compared to those of other natural fibers [13, 28, 38]

Fiber name	Diameter (μm)	Tensile strength (MPa)	Modulus (GPa)	BRK.%STN (%)
Windmill palm leaf sheath				
Inner layer	202.1	113.72	1.25	39.52
Middle layer	418.0	91.93	0.78	55.20
Outer layer	342.5	82.08	0.82	47.52
Banana	80–250	529–759	8–20	1–3.5
Elephant grass	70–400	185	7.40	2.50
Sea-grass (*Zostera marina*)	4.6	573 ± 120	19.8 ± 6.8	3.4 ± 0.3
Flax	17.8	1339 ± 486	58 ± 15	3.3 ± 0.8
Hemp	10–50	389	35	1.6
Jute	25–200	393–773	26.5	1.5–1.8
Sisal	7–47	350–700	9–21	3–7
Coconut palm				
Leaf sheath (inside top)	300–600	88.63	2.45	14.22
Leaf sheath (thick fibers)	1100–1600	115.24	4.54	3.97
Leaf sheath (middle fibers)	300–1000	91.97	3.59	6.227
Bark of the petiole	250–550	185.52	15.09	2.06
Root	100–650	157	6.2	3
Coir	100–450	131–175	4–6	15–40

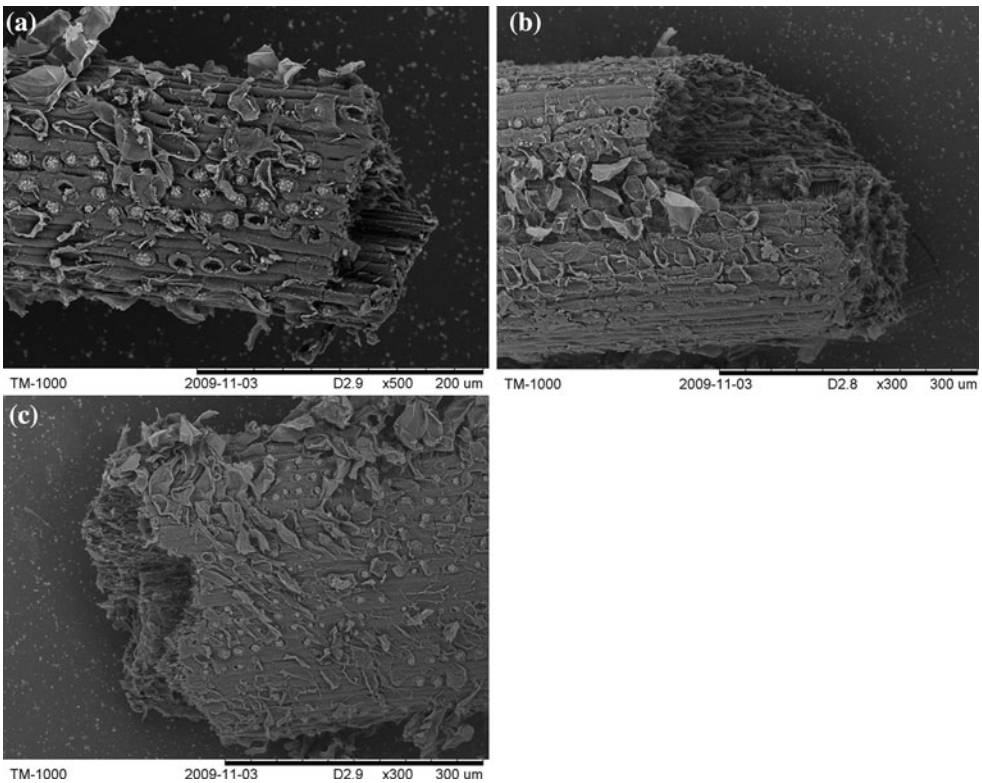

Fig. 12 Fracture surface of fiber bundles taken from inner (**a**), middle (**b**), and outer layers (**c**) of one sheet of windmill palm leaf sheath

Table 4 Microfibril angles (MFA), relative crystallinity index (CrI), and recalculated data of fiber bundles

Layers	MFA	CrI	$S_V/(S_V + S_F)$ (%)	Tensile strength[a] (MPa)
Inner	38.5	0.71	6	171.2
Middle	37.8	0.73	33	179.1
Outer	42.2	0.67	32	127.3

[a] Excluding the S_V area and recalculating tensile strength using the effective area (S_F)

Martinschitz et al. [36], the formation of curled triangular features is related to the fracture of individual helical cells, which indicates a specific fracture mechanism.

Microfibril angle analysis

Excluding S_V area and recalculating tensile strength only using the effective area (S_F) revealed that inner-layer fiber bundles and middle-layer fiber bundles have a similar degree of tensile strength. However, the tensile strength of the outer-layer fiber bundles was lower, showing 127.3 MPa (Table 4). These data indicate that the structure of the outer-layer fiber bundles might differ from that of the other two layers.

Figure 13 shows the wide-angle X-ray scattering (WAXS) patterns of fiber bundles in the different layers of one sheet of leaf sheath. Apparently it is difficult to detect a difference in MFA of the major cell wall layer. The data listed in Table 4 were obtained from profile analysis. Although we do not have statistical data, results of MFA showed opposite rank of recalculated tensile strength according to the position of fiber bundles. The MFA data and tensile strength measurements for windmill palm fiber bundles conformed to the same principle previously observed in wood by researchers; namely, the lower the microfibril angle, the higher the modulus of elasticity and tensile strength of both wood tissues and individual wood fibers [40–44].

As seen in Table 4's list of mechanical properties, the inner layer had significantly smaller values in comparison to the other two layers. The difference is so large that the MFA could not be due only to poor mechanical properties. Other factors, such as matrix and/or cell wall architecture, also seemed to be responsible. In addition, we measured the chemical constituents of fiber bundles from the different layers of the windmill palm. According to chemical analysis results, there was no significant difference in fiber bundles from the different layers, which again supports the above contention that matrix and/or cell wall architecture are responsible for a fiber bundle's mechanical properties.

It is interesting that the fiber bundles in one sheet of leaf sheath showed different tensile strength and that MFA values also varied. A similar difference in the scales of seed-bearing pine cones was found by Dawson et al. [45]. A scale consists of two tissues, which differ greatly in their tensile stiffness. Pine cone scales move in response to changes in relative humidity, which results in the release of the cone's seeds. Researchers have concluded that the mechanism of the bending of the scales depends on the way in which the orientation of cellulose microfibrils controls the hygroscopic expansion of the cells. An arrangement of tissues and cells with cell walls of different orientations of cellulose fibrils can be utilized for adjusting mechanical properties and controlling specific movements of organs as shown for wood, pine cones, and wheat awns [44, 46]. Consequently, complex movements caused by the swelling or shrinking of cell walls are achieved by having cell wall architecture with well ordered cellulose fibrils. In the windmill palm, the varying MFA in one sheet of leaf sheath might be related to the biomechanical movements of organs, such as development of a criss-cross structure and expansion of leaf sheaths.

Conclusion

Fiber bundles taken from a mature windmill palm leaf sheath can be divided into three groups according to their size, orientation, and location in one sheet of leaf sheath: *inner*, *middle*, and *outer* layers. The diameter of fiber bundles in the *middle* layer was the largest, while the diameter of those in

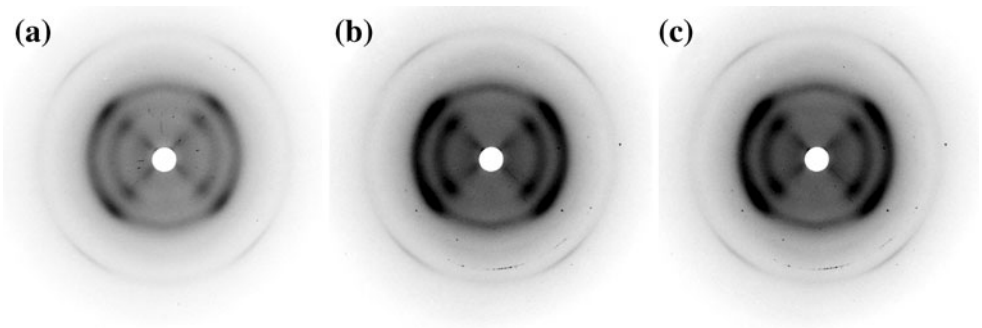

Fig. 13 Result from WAXS on fiber bundles taken from inner (**a**), middle (**b**), and outer layers (**c**) of one sheet of windmill palm leaf sheath

the *inner* layer was the smallest. Tensile strength and Young's modulus showed a decreasing tendency with an increasing diameter of these fiber bundles. S_V and S_F were measured by observing transmitted- and polarized-light photomicrographs of fiber bundles from the three layers. The ratio of S_V versus transverse sectional area in the inner layer was just 6%, while that in the middle layer was 33%. These findings strongly suggest that fiber bundle tensile strength increases in parallel with a decrease of S_V, while the presence of fibers predominantly contributes to mechanical strength. Therefore, the fiber bundles in the inner layer were stronger that those in the middle layer.

Excluding S_V area and recalculating tensile strength using S_F revealed that the tensile strength of the outer-layer fiber bundles was lower than that of the inner and middle layer fiber bundles. The MFA data of the three layers followed the principle observed in wood; namely, that the lower the microfibril angle, the higher the tensile strength. Indeed, the varying MFA in one sheet of leaf sheath might be related to the biomechanical movements of leaf sheath in the windmill palm—a topic worthy of further exploration.

Acknowledgements The authors would like to thank Prof. Masahisa Wada's laboratory in The University of Tokyo's Department of Biomaterials Science for the assistance it provided in measuring X-ray diffraction. The authors are also grateful to Prof. Shuichi Kawai's laboratory in Kyoto University's Research Institute for Sustainable Humanosphere for the help it gave with mechanical properties testing. Dr. Mechtild Mertz of the Research Institute for Nature and Humanity kindly offered feedback and answered questions about language usage. Author Shengcheng Zhai wishes to thank the G30 Program of Kyoto University's Faculty of Agriculture and the Kambayashi Scholarship Foundation for their generous financial support.

References

1. Tomlinson PB (1961) Anatomy of the monocotyledons. II. PALMAE. Oxford University Press, London
2. Whitmore TC (1977) Palms of Malaya. Oxford University Press, Oxford
3. Frederick BE, Dong Y (1987) Econ Bot 41(3):411
4. Tomlinson PB (1990) The structural biology of palms. Oxford University Press, USA
5. Pei S, Chen S, Tong S (1991) Tomus13(1): Angiospermae–Monocotyledoneae, Palme, Flora of Reipublicae *Popularis Sinicae*. Science Press, Beijing
6. Harries HC (1978) Bot Rev 44(3):265
7. Dassanayake MD, Sivakadachcham B (1974) Phytomorphology 22(3–4):296
8. Hartley CWS (1967) The oil palm (*Elaeis guineensis* Jacq.). Longman Scientific and Technical, England
9. Sreenivasan S, Bhama Iyer P, Krishna Iyer KR (1996) J Mater Sci 31(3):721. doi:10.1007/BF00367891
10. Sreekala MS, Kumaran MG, Thomas S (1998) J Appl Polym Sci 66(5):821
11. Hill CAS, Abdul Khalil HPS (2000) J Appl Polym Sci 78(9):1685
12. Matthes M, Singh R, Cheah SC, Karp A (2001) TAG Theor Appl Genet 102(6–7):971
13. Satyanarayana KG, Pillai CKS, Sukumaran K, Pillai SGK (1982) J Mater Sci 17:2453. doi:10.1007/BF00543759
14. Sreekala MS, George J, Kumaran MG, Thomas S (2002) Compos Sci Technol 62(3):339
15. Sreekala MS, Thomas S (2003) Compos Sci Technol 63(6):861
16. Jacob M, Thomas S, Varughese KT (2004) Compos Sci Technol 64(7–8):955
17. Abu-Sharkh B, Rychlý J, Matisová-Rychlá L (2005) J Mater Sci 40:613. doi:10.1007/s10853-005-6298-5
18. Windsor-Collins AG, Atherton MA, Collins MW, Cutler DF (2008) Int J Des Nat Ecodyn 3(3):190
19. Li S (2008) Bencao gangmu (1578)—compendium of materia medica. Science and Technology Publishing, Shanghai (in Chinese)
20. Nanjing Municipal Museum (2006) Ming dynasty Baochuanchang Shipyard in Nanjing. Cultural Relics Publishing House, Beijing (in Chinese)
21. Itoh T, Mertz M, Pan B, Luo J (2008) Wood identification of excavated wooden artifacts in underwater site near Takashima island of Matsuura-city, second report of the cultural properties of Matsuura-city. Report of emergency excavations following Kamizaki harbor repair works 2001 to 2002. Board of Education of Matsuura city, Nagasaki prefecture (in Japanese)
22. Zhang M, Kishimmoto Y, Kawai S, Sasaki H (1994) Wood Res Tech Notes (Kyoto Univ.) 30:32
23. Munawar SS, Umemura K, Kawai S (2007) J Wood Sci 53:108
24. Rüggeberg M, Speck T, Paris O, Lapierre C, Pollet B, Koch G, Burgert I (2008) Proc R Soc B275:2221
25. Rüggeberg M, Speck T, Burgert I (2009) New Phytol 182:443
26. Smole MS, Krež T, Strnad S, Kleinschek KS, Hribernik S (2005) J Mater Sci 40:5349. doi:10.1007/s10853-005-4298-0
27. American Society for Testing, Materials (1978) ASTM D 3379–75 standard test method for tensile strength and Young's modulus for high-modulus single-filament materials. ASTM, Philadelphia, p 847
28. Rao KMM, Prasad AVR, Babu MNVR, Rao KM, Gupta AVSSKS (2007) J Mater Sci 42:3266. doi:10.1007/s10853-006-0657-8
29. Wada M, Okano T, Sugiyama J, Horii F (1995) Cellulose 2:223
30. Kim DY, Nishiyama Y, Kuga S (2002) Cellulose 9:361
31. Noishiki Y, Nishiyama Y, Wada M, Kuga S, Magoshi J (2002) J Appl Polym Sci 86(13):3425
32. Hori R, Wada M (2005) Cellulose 12:479
33. Wada M, Heux L, Sugiyama J (2004) Biomacromolecules 5(4):1385
34. Wang Y, Leppänen K, Andersson S, Serimaa R, Ren H, Fei B (2011) Studies on the nanostructure of the cell wall of bamboo using X-ray scattering. Wood Sci Technol. doi:10.1007/s00226-011-0405-3
35. Carr DJ, Cruthers NM, Lains RM, Niven BE (2006) J Mater Sci 41:511. doi:10.1007/s10853-005-2189-z
36. Martinschitz KJ, Boesecke P, Garvey CJ, Gindl W, Keckes J (2008) J Mater Sci 43:350. doi:10.1007/s10853-006-1237-7
37. Baley C (2002) Composites A 33:939
38. Davies P, Morvan C, Sire O, Baley C (2007) J Mater Sci 42:4850. doi:10.1007/s10853-006-0546-1
39. Yu Y, Jiang Z, Fei B, Wang G, Wang H (2011) J Mater Sci 46:739. doi:10.1007/s10853-010-4806-8
40. Cave ID, Hutt L (1969) Wood Sci Technol 3:40
41. Reiterer A, Lichtenegger H, Tschegg S, Fratzl P (1999) Philos Mag A 79(9):2173
42. Burgert I, Keckes J, Frühmann K, Fratzl P, Tschegg SE (2002) Plant Biol 4(1):9
43. Groom L, Mott L, Shaler S (2002) Wood Fiber Sci 34(1):14
44. Burgert I, Fratzl P (2009) Integr Comp Biol 49(1):69
45. Dawson C, Vincent JFV, Rocca AM (1997) Nature 390:668
46. Elbaum R, Zaltzman L, Burgert I, Fratzl P (2007) Science 316:884